from radical-induced cleavage. In order to assess the time and domain dependence of such cleavage, we quantified cleavages over specific regions and plotted these as a fraction of relative protection versus time (Figure 2b). This analysis suggests that individual domains of the ribozyme assemble at different rates (Figure 2c) and is consistent with the results of both synchrotron X-ray footprinting[11] and an oligonucleotide hybridization/cleavage assay,[17] two other methods that have been used to analyze the folding pathway of the *Tetrahymena* ribozyme. The P4-P6 region is protected very quickly during the folding process and has been proposed as a scaffold around which other folding events take place.[18] Assembly of the P3 helix at the core of the catalytic domain is a late-occurring event and may be reflective of kinetic traps along the folding pathway.[19]

The formation of the P4 helix clearly occurs too fast to be measured with the peroxynitrous acid reagent—analysis of events such as these requires the more rapid radical generation available through synchrotron irradiation. However, formation of the P3 helix is significantly slower. This event takes place with a first-order rate constant (k_{P3} 0.09 s^{-1}); the half-time for protection is roughly eight seconds. A comparison with the overall rate of folding (Figure 1b) indicates that P3 formation is not the rate determining step—we are carrying out additional investigations, including an analysis of the rates of folding of other regions of the ribozyme.

Our results with the *Tetrahymena* system validate the use of peroxynitrous acid as a kinetic footprinting tool; this easily used methodology should prove valuable in the elucidation of many relatively slow RNA folding pathways and the examination of RNA dynamics in complex systems.

Experimental Section

Potassium peroxynitrite synthesis: HCl (0.5 M, 5 mL) was added to a stirred ice-cooled aqueous solution (10 mL) containing $NaNO_2$ (0.6 M, 0.41 g) and H_2O_2 (3%). A solution (5 mL) containing diethylenetriaminepentaacetic acid (400 μM, 3.3 mg) and KOH (1.6 M) was added immediately afterwards. The resulting mixture was stirred for 5 minutes then MnO_2 (100 mg) was added and stirring continued for 20 minutes. Excess MnO_2 was removed by gravity filtration (performed at 4 °C). Typical yields of potassium peroxynitrite were 80–130 mM measured by UV absorbance at 302 nm (ε = 1670 $M^{-1}cm^{-1}$). Even a slight delay in the addition of the KOH/diethylenetriaminepentaacetic acid solution resulted in significantly lower yields of potassium peroxynitrite. The potassium peroxynitrite solution was stored at −78 °C with no decrease in concentration after 10 weeks.

Peroxynitrous acid footprinting: L-21 Group I ribozyme folding was initiated by the addition of $MgCl_2$ (final concentration 10 mM) to a solution (final volume 20 μL) containing final concentrations of NaCl (80 mM), NaH_2PO_4/Na_2HPO_4 (50 mM, pH 7), 5′-end labeled ribozyme (50 nM, 3×10^6 cpm) at 22 °C. Footprinting was then effected by the addition of potassium peroxynitrite (1 μL, 130 mM) at the indicated times (see Figure 2). Footprinting reactions were allowed to proceed for 20 seconds before freezing on dry ice, followed by ethanol precipitation. Reactions (1×10^6 cpm) were then subjected to denaturing polyacrylamide gel electrophoresis (PAGE, 6%, 19:1) for 2.3 hours at 85 W. Dried gels were exposed to a molecular dynamics phosphor screen, which was then scanned on a Molecular Dynamics Storm 860 Phosphorimager. To calculate the fractional peroxynitrous acid protection (footprint), the background intensity (ImageQuant 5.0) was first subtracted and a correction for differences in lane loading was applied. The intensity of a region at a given time was divided by the intensity of the same region at time zero. The resulting fractional intensities were normalized from 0 to 1. Plots of normalized fractional protection versus folding time were fitted to a first-order exponential (GraFit 3.00) using data averaged from five separate experiments.

Received: July 26, 1999 [Z13782]

[1] See *The RNA world*, 2nd ed. (Eds.: R. F. Gesteland, T. R. Cech, J. F. Atkins), Cold Spring Harbor Laboratory, Cold Spring Harbor, **1999**.
[2] F. Michel, E. Westhof, *J. Mol. Biol.* **1990**, *216*, 585–610.
[3] J. H. Cate, A. R. Gooding, E. R. Podell, K. Zhou, B. L. Golden, C. E. Kundrot, T. R. Cech, J. A. Doudna, *Science* **1996**, *273*, 1678–1685.
[4] B. L. Golden, A. R. Gooding, E. R. Podell, T. R. Cech, *Science* **1998**, *282*, 259–264.
[5] W. G. Scott, *Curr. Opin. Struct. Biol.* **1998**, *8*, 720–726.
[6] M. Wu, I. Tinoco, Jr., *Proc. Natl. Acad. Sci. USA* **1998**, *95*, 11555–11560.
[7] A. A. Szewczak, L. Ortoleva-Donnelly, S. P. Ryder, E. Moncoeur, S. A. Strobel, *Nat. Struct. Biol.* **1998**, *5*, 1037–1042.
[8] R. T. Batey, R. P. Rambo, J. A. Doudna, *Angew. Chem.* **1999**, *111*, 2472–2491; *Angew. Chem. Int. Ed.* **1999**, *38*, 2326–2343.
[9] J. A. Latham, T. R. Cech, *Science* **1989**, *245*, 276–282.
[10] C.-H. B. Chen, D. S. Sigman, *J. Am. Chem. Soc.* **1988**, *110*, 6570–6572.
[11] a) B. Sclavi, S. A. Woodson, M. Sullivan, M. R. Chance, M. Brenowitz, *J. Mol. Biol.* **1997**, *266*, 144–159; b) B. Sclavi, M. Sullivan, M. R. Chance, M. Brenowitz, S. A. Woodson, *Science* **1998**, *279*, 1940–1943.
[12] C. E. Richeson, P. Mulder, V. W. Bowry, K. U. Ingold, *J. Am. Chem. Soc.* **1998**, *120*, 7211–7219.
[13] P. A. King, V. E. Anderson, J. O. Edwards, G. Gustafson, R. C. Plumb, J. W. Suggs, *J. Am. Chem. Soc.* **1992**, *114*, 5430–5432.
[14] P. A. King, E. Jamison, D. Strahs, V. E. Anderson, M. Brenowitz, *Nucleic Acids Res.* **1993**, *21*, 2473–2478.
[15] M. Götte, R. Marquet, C. Isel, V. E. Anderson, G. Keith, H. J. Gross, B. Ehresmann, H. Heumann, *FEBS Lett.* **1996**, *390*, 226–228.
[16] J. S. Beckman, T. W. Beckman, J. Chen, P. A. Marshall, B. A. Freeman, *Proc. Natl. Acad. Sci. USA* **1990**, *87*, 1620–1624.
[17] P. P. Zarrinkar, J. R. Williamson, *Science* **1994**, *265*, 918–924.
[18] E. A. Doherty, J. A. Doudna, *Biochemistry* **1997**, *36*, 3159–3169.
[19] M. S. Rook, D. K. Treiber, J. R. Williamson, *J. Mol. Biol.* **1998**, *281*, 609–620.

Solvation of the Carbonyl Compound as a Predominant Factor in the Diastereofacial Selectivity of Nucleophilic Addition**

Gianfranco Cainelli,* Paola Galletti, Daria Giacomini,* and Paolo Orioli

Discussions of factors controlling stereoselectivity commonly focus on steric and/or electronic features of the catalyst and/or the substrate.[1] However, selectivity is a kinetic

[*] G. Cainelli, D. Giacomini, P. Galletti, P. Orioli
Dipartimento di Chimica "G. Ciamician"
Via Selmi 2, 40126 Bologna (Italy)
Fax: (+390) 51-209-9456
E-mail: cainelli@ciam.unibo.it, giacomin@ciam.unibo.it

[**] This work was supported by MURST and the University of Bologna (Fund for Selected Topics). We thank Andrea Garelli for assistance with the NMR spectroscopy.

phenomenon governed by the ratio of the rate of formation for one stereoisomer with respect to that of the other. The stereoselectivity can be influenced not only by varying the reactants but also by changing the reaction conditions. In this perspective, reaction temperature and solvent are readily available parameters for controlling selectivity.

Solvents play a critical role in chemical processes: both equilibrium constants and reaction rates may change drastically in different solvents.[2] There are examples of the effect of solvent on face selectivity in which a variation of the diastereomeric excess is observed and others in which a complete reversal of diastereoselectivity occurs because of a change in the reaction solvent.[3] We believe that the influence of solvent on diastereomeric excess can be considered a macroscopic effect arising from molecular, microscopic solute–solvent interactions which differently affect the two reaction paths leading to the diastereomers. The description, from a microscopic point of view, of solvation processes and of their effects on the energetics and dynamics of chemical reactions constitutes a general topic of main relevance, but research in this field is still only at the beginning.[4]

The effect of temperature on diastereoselectivity has long been observed and its influence is not uniform: on increasing the reaction temperature the diastereoselectivity may decline, but it may be constant or even increase. Analysis of the logarithmic values of the isomer ratio (S) as a function of the reciprocal temperature results in the linear relationship shown in Equation (1), where $S = k/k' = I/I'$, k, k' are the overall rate constants, and I, I' are the relative amounts of the *anti* and the *syn* isomer, respectively.

$$\ln S = -(\Delta\Delta H^{\neq}/RT) + (\Delta\Delta S^{\neq}/R) \quad (1)$$

According to Eyring's theory,[5] when this relationship is plotted, the slope corresponds to the difference in the overall activation enthalpies and the intercept represents the difference in the overall activation entropies. However, for some reactions a nonlinear plot is obtained. In these cases, the corresponding Eyring plots generally consist of two linear regions intersecting at a so-called inversion temperature (T_{inv}). This phenomenon was reviewed in 1991 by Scharf et al.,[6] and in the meantime other processes with a nonlinear relationship between stereoselectivity and reaction temperature have been described.[7]

In recent papers we have formulated the idea that a sort of phase modification occurs at T_{inv}.[8] In our hypothesis the inversion temperature could constitute a transition between two different solvation states that could be described as two different solute–solvent clusters with a different order.[9] These supramolecular structures behave like different molecules and produce a measurable change in thermodynamic properties and therefore in diastereoselectivity. In this hypothesis T_{inv} represents the interconversion temperature between two supramolecules, and it does not imply any change either in the rate-determining step or in the reaction mechanism.

In the present investigation we report preliminary results that strengthen our proposal on the solvation of carbonyl compounds as the predominant factor in the nonlinear effect of temperature on diastereofacial selectivity. In fact, we report evidence that T_{inv} does not depend on nucleophiles, and that its value can be obtained from a ^{13}C NMR experiment in which the change in the C=O chemical shift versus temperature is recorded.

(2*S*)-*O*-(*tert*-Butyldimethylsilyl)lactic aldehyde (**1**), (2*S*)-*O*-(*tert*-butyldimethylsilyl)mandelic aldehyde (**2**), and (2*S*)-*O*-(triisopropylsilyl)lactic aldehyde (**3**) were allowed to react with *tert*-butyllithium and *n*-butyllithium in THF and *n*-hexane, and with *n*-butylmagnesium bromide in THF to give the corresponding *anti* and *syn* monoprotected diols (Scheme 1). The addition reactions were performed by adding

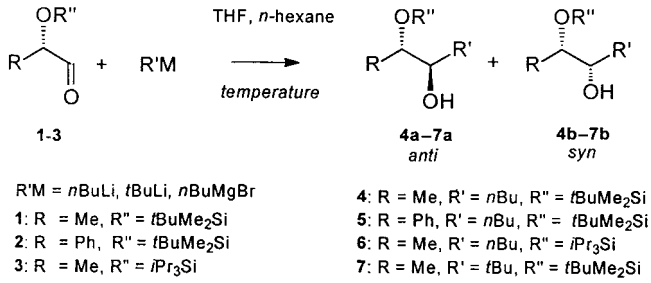

1-3 **4a–7a** *anti* **4b–7b** *syn*

R'M = *n*BuLi, *t*BuLi, *n*BuMgBr
1: R = Me, R'' = *t*BuMe$_2$Si
2: R = Ph, R'' = *t*BuMe$_2$Si
3: R = Me, R'' = *i*Pr$_3$Si
4: R = Me, R' = *n*Bu, R'' = *t*BuMe$_2$Si
5: R = Ph, R' = *n*Bu, R'' = *t*BuMe$_2$Si
6: R = Me, R' = *n*Bu, R'' = *i*Pr$_3$Si
7: R = Me, R' = *t*Bu, R'' = *t*BuMe$_2$Si

Scheme 1. Formation of the *anti* and *syn* monoprotected diols.

a stoichiometric amount of the organometallic reagent dropwise to a solution of the pure aldehyde in dry THF or *n*-hexane. The reaction was conducted at temperatures ranging over 150 °C. The diastereomeric excess of the products was determined by GC analysis.[10] The results were elaborated in the corresponding Eyring plots. The data have been treated by the least-squares method to obtain linear relationships. Each aldehyde–solvent combination gave plots with two linear regions in the temperature range explored, and in all cases we determined the characteristic T_{inv} value (Table 1).

Table 1. Inversion temperatures (T_{inv}) for the addition of *n*BuLi, *t*BuLi, and *n*BuMgBr to aldehydes **1**–**3** in *n*-hexane and THF as well as the ^{13}C NMR break temperatures (T_{NMR}) in the linear variation of $\delta(^{13}C{=}O)$ versus temperature.

Aldehyde/RM′	Solvent	T_{inv} [°C]	Aldehyde	Solvent	T_{NMR} [°C]
1/*n*BuLi	*n*-hexane	−83	**1**	[D$_{14}$]*n*-hexane	−68
1/*t*BuLi	*n*-hexane	−81			
1/*n*BuLi	THF	−12	**1**	[D$_8$]THF	0
1/*n*BuMgBr	THF	+1			
1/*t*BuLi	THF	−13			
2/*n*BuLi	THF	−63	**2**	[D$_8$]THF	−47
2/*n*BuMgBr	THF	−65			
3/*n*BuLi	THF	−46	**3**	[D$_8$]THF	−42

The diastereofacial selectivity of *n*BuLi addition to lactic aldehyde **1** in *n*-hexane is only slightly temperature sensitive. Nevertheless, T_{inv} is quite evident at −83 °C (Figure 1a). With *t*BuLi the selectivity is notably affected and increases with reducing temperature. Interestingly, both plots exhibit quite similar inversion temperatures.

The reactions with *t*BuLi and *n*BuLi in THF at low temperature give divergent plots on account of the opposite temperature effect on the selectivity (Figure 1b). The diastereofacial selectivity in the addition of *n*BuMgBr to **1** is less

  0570-0833/00/3903-0524 $ 17.50+.50/0 *Angew. Chem. Int. Ed.* **2000**, *39*, No. 3

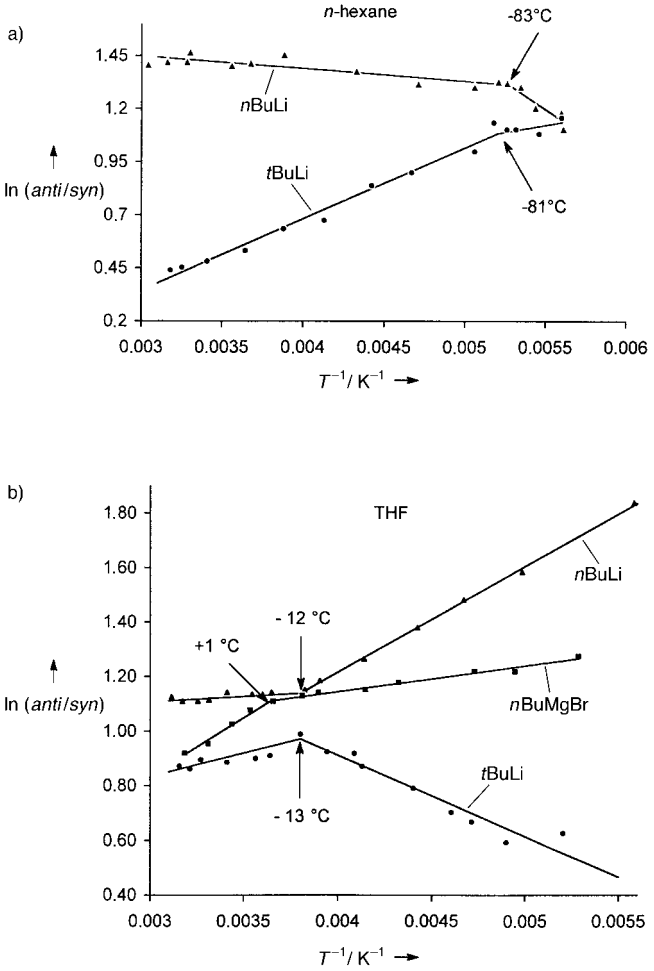

Figure 1. Eyring plots for the *anti/syn* ratio of the diastereomers formed from the nucleophilic addition of *n*-butyllithium (▲), *tert*-butyllithium (●), and *n*-butylmagnesium bromide (■) to **1** at various temperatures in *n*-hexane (a) and THF (b).

affected by temperature than the organolithium reactions. In this case T_{inv} is $+1\,^{\circ}C$. The plots are more differentiated at low temperature with *t*BuLi, *n*BuLi, and *n*BuMgBr. Remarkably, all three plots in Figure 1 show T_{inv} values in a narrow temperature range.

In the next set of experiments *n*BuMgBr and *n*BuLi were added to mandelic aldehyde **2** (Figure 2). Both plots reach negative values of ln (*anti/syn*); thus, it is possible to invert the diastereofacial selectivity by means of reaction temperature. Despite the slight change in selectivity with temperature, these two plots have a very similar T_{inv} value (-65 and $-63\,^{\circ}C$, respectively).

In nucleophilic addition reactions of this type, temperature and solvent effects on the diastereomeric excess might be ascribed to the presence of different organometallic species in solution.[11] However, the dynamic process that involves the aggregation state of the organometallic reagent acts before the reacting event (C–C bond formation) so that the corresponding rate constants are identical for the reaction paths that lead to both *syn* and *anti* diastereomers. Thus, a mere ground-state effect would be irrelevant. The tendency of organometallic species to aggregate may to some extent influence the structure of the transition states. Moreover, we found that different organometallic reagents with different molecular structures in solution have similar inversion temperatures. Thus, the influence of aggregation and solvation of the organometallic compound on stereoselectivity is limited by the kinetic expression of selectivity ($S = k/k'$),[12] where in the ratio of overall kinetic constants all the equal terms vanish. All the above results clearly show that T_{inv} is greatly dependent on the aldehyde–solvent combination and less on the nucleophile. This fact emphasizes our idea that the solvation of the starting carbonyl compound accounts for the T_{inv} value.

NMR techniques provide a powerful method for investigating the local electronic environment of the molecular structure, and nuclear shielding is a sensitive probe of intermolecular interactions and solvent effects.[13] In this study we conducted a series of ^{13}C NMR experiments in deuterated THF and *n*-hexane with aldehydes **1**–**3** to determine whether the chemical shift is temperature dependent. Figure 3a displays the change in the C=O ^{13}C chemical shift as a function of temperature in $[D_{14}]$*n*-hexane for aldehyde **1**. This result can be directly compared with the Eyring plot for the reaction of same aldehyde with *n*BuLi in THF (Figure 1).

The ^{13}C chemical shift of C=O in aldehyde **1** decreased on warming. This effect could be the result of a loss of electron density near the observed nucleus. On further checking the experimental data points we recognized a break in the linear variation of chemical shift versus temperature. We applied the least median squares (LMS) regression to determine the *T* value of these breaks more precisely.[14] Use of the LMS regression improves the reliability and the ability to objectively define the segments of the straight line given by experimental data. Table 1 lists the break temperatures for the substrates studied. These temperature values change with the solvent and the substrate and, surprisingly, they correspond or are fairly close to the inversion temperatures obtained with the same substrate–solvent combination in the nucleophilic addition reaction.

This result reinforces our hypothesis that T_{inv} corresponds to a transition between two differently ordered solvation states. As we stated earlier the inversion temperature reflects

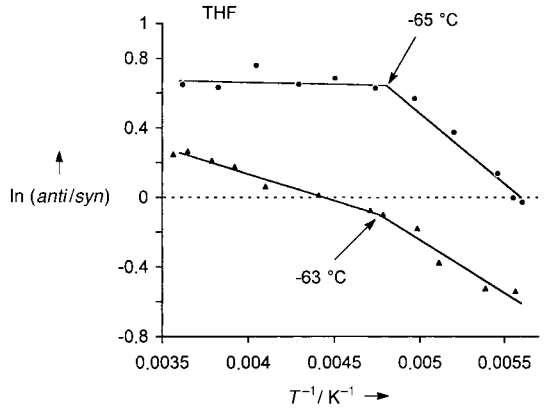

Figure 2. Eyring plots for the *anti/syn* ratio of the diastereomers formed from the nucleophilic addition of *n*-butyllithium (▲) and *n*-butylmagnesium bromide (●) to **2** at various temperatures in THF.

  0570-0833/00/3903-0525 $ 17.50+.50/0

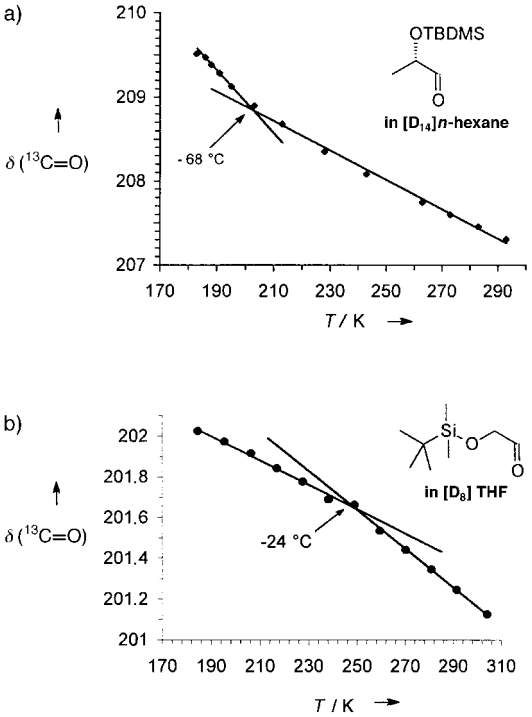

Figure 3. Plots of $\delta(^{13}C{=}O)$ versus temperature for **1** in deuterated *n*-hexane (a) and for 2-(*tert*-butyldimethylsilyloxy)ethanal in deuterated THF (b). Solid lines are the fitting results. See text for details on the line fitting. TBDMS = *tert*-butyldimethylsilyl.

the solvation state of the carbonyl compound. Changes in the solvation state with the temperature can be not continuous, and it makes an abrupt change corresponding to the T_{inv} value. Because of its very nature this phenomenon should not be tied to the presence of a stereocenter in the carbonyl compound. In fact, the plot in Figure 3b shows the change in the ^{13}C chemical shift of C=O for 2-*(tert*-butyldimethylsilyloxy)ethanal in deuterated THF, and it shows a break at $T = -24\,^{\circ}C$. This achiral aldehyde has a change in its solvation shell that could affect its reactivity simply because two different solvation clusters exist in the two temperature regions and act as two different molecules. This result challenges us to find a reaction that will show nonlinear selectivity with temperature and a T_{inv} value close to the break temperature revealed in the ^{13}C NMR experiment.

We have demonstrated that the inversion temperature observed in Eyring plots obtained for diastereoselective nucleophilic additions to α-chiral aldehydes does not depend on nucleophiles. The ^{13}C NMR results clearly connect the phenomenon of T_{inv} with the solvation of the starting carbonyl compound, and they shed light on nonlinear temperature effects on stereoselectivity. This confirms our earlier hypothesis of the solvent-dependent nature of T_{inv}.

Experimental Section

The ^{13}C chemical shift measurements were made with a Varian Gemini 300 instrument operating at 75.5 MHz using a 5-mm probe. All chemical shifts are quoted relative to signals of the deuterated solvent. The temperature was controlled by a variable-temperature unit using the flow of temperature-regulated nitrogen gas. The temperature was calibrated from differences in the chemical shift of a methanol sample.[15] The *anti/syn* ratios and the *de* values were obtained from GC analysis of the crude products or of the corresponding *O*-trimethylsilyl-derivatives. The average standard deviation for the *de* measurements was less than 1%.

In a typical experiment, the aldehyde (1 mmol) was dissolved in anhydrous solvent (20 mL) under an inert atmosphere, and the solution was cooled or warmed to the desired temperature. Then *n*-butyllithium, *tert*-butyllithium, or *n*-butylmagnesium bromide (1.2 mmol) was added. After the starting aldehyde had disappeared (GC monitoring), the reaction mixture was quenched with a saturated aqueous solution of NH_4Cl and extracted with CH_2Cl_2 (3×50 mL), and the extracts were dried with Na_2SO_4 and concentrated to dryness. Chromatography of the residue on a silica gel column gave a mixture of alcohols **4a**–**7a** and **4b**–**7b**. The calculated chemical yields ranged from 80 to 90%. After removal of the tBuMe$_2$Si group by means of Bu_4NF in THF, the configuration of the 1,2-diol was determined by comparison with reported data.[16]

Received: June 9, 1999 [Z13537]

[1] For a review on classical conformational models, see E. L. Eliel, S. H. Wilen, L. N. Mander, *Stereochemistry of Organic Compounds*, Wiley, New York, **1994**, p. 875; R. E. Gawley, J. Aubé, *Principles of Asymmetric Synthesis*, Pergamon, Oxford, **1996**.

[2] C. Reichardt, *Solvents and Solvent Effects in Organic Chemistry*, 2nd ed., VCH, Weinheim, **1990**.

[3] See for example: N. Hoffmann, H. Buschmann, G. Raabe, H.-D. Scharf, *Tetrahedron* **1994**, *50*, 11167; G. Cainelli, D. Giacomini, F. Perciaccante, *Tetrahedron*: *Asymmetry* **1994**, *5*, 1913; Y. Inoue, N. Yamasaki, T. Yokoyama, A. Tai, *J. Org. Chem.* **1992**, *57*, 1332; D. Awandi, F. Henin, J. Muzart, J.-P. Pete, *Tetrahedron*: *Asymmetry* **1991**, *2*, 1101.

[4] D. J. Giesen, C. J. Cramer, D. G. Truhlar, *J. Phys. Chem.* **1995**, *99*, 7137; G. D. Hawkins, D. A. Liotard, C. J. Cramer, D. G. Truhlar, *J. Org. Chem.* **1998**, *63*, 4305; M. F. Ruiz-Lopez, X. Assfeld, J. I. Garcia, J. A. Mayoral, L. Salvatella, *J. Am. Chem. Soc.* **1993**, *115*, 8780; M. Sola, A. Lledos, M. Duran, J. Bertran, J.-L. M. Abboud, *J. Am. Chem. Soc.* **1991**, *113*, 2873.

[5] H. Eyring, *J. Phys. Chem.* **1935**, *3*, 107; S. Glasstone, K. J. Laidler, H. Eyring, *The Theory of Rate Processes*, McGraw-Hill, New York, **1941**, Chap. 4.

[6] H. Buschmann, H.-D. Scharf, N. Hoffmann, P. Esser, *Angew. Chem.* **1991**, *103*, 480; *Angew. Chem. Int. Ed. Engl.* **1991**, *30*, 477.

[7] For recent papers, see K. J. Hale, J. H. Ridd, *J. Chem. Soc. Perkin Trans. 2* **1995**, 1601; J. Muzart, F. Hénin, S. J. Aboulhoda, *Tetrahedron*: *Asymmetry* **1997**, *8*, 381; M. Palucki, P. J. Pospisil, W. Zhang, E. N. Jacobsen, *J. Am. Chem. Soc.* **1994**, *116*, 9333; J. Brunne, N. Hoffmann, H.-D. Scharf, *Tetrahedron* **1994**, *50*, 6819; T. Göbel, K. B. Sharpless, *Angew. Chem.* **1993**, *105*, 1417; *Angew. Chem. Int. Ed. Engl.* **1993**, *32*, 1329; J. Muzart, F. Hénin, J.-P. Pète, A. M'boungou-M'Passi, *Tetrahedron*: *Asymmetry* **1993**, *4*, 2531; I. Tóth, I. Guo, B. E. Hanson, *Organometallics* **1993**, *12*, 477.

[8] G. Cainelli, D. Giacomini, P. Galletti, A. Marini, *Angew. Chem.* **1996**, *108*, 3016; *Angew. Chem. Int. Ed. Engl.* **1996**, *35*, 2849; G. Cainelli, D. Giacomini, P. Galletti, *Eur. J. Org. Chem.* **1999**, 61; G. Cainelli, D. Giacomini, P. Galletti, *Chem. Commun.* **1999**, 567.

[9] Partial ordering of molecules is possible in solution, and a temperature-dependent change in this order is already manifested in the nonlinearity of some spectroscopic properties. See for instance: J. B. Robert, *Mol. Phys.* **1997**, *90*, 399; M. A. Wendt, J. Meiler, F. Weinhold, T. C. Farrar, *Mol. Phys.* **1998**, *93*, 145.

[10] GC analyses were carried out on a HRGC 5300 Carlo Erba instrument using a OV 1701 (25 m) column with a chiral phase.

[11] J. F. McGarrity, C. A. Ogle, *J. Am. Chem. Soc.* **1984**, *107*, 1805; J. F. McGarrity, C. A. Ogle, Z. Brich, H.-R. Loosli, *J. Am. Chem. Soc.* **1984**, *107*, 1810.

[12] D. Heller, H. Buschmann, *Top. Catal.* **1998**, *5*, 159.

[13] For solvent effects on chemical shift see for instance: T. Helgaker, M. Jaszunski, K. Ruud, *Chem. Rev.* **1999**, *99*, 293; E. Y. Lau, J. T. Gerig, *J. Am. Chem. Soc.* **1996**, *118*, 1194; E. Y. Lau, J. T. Gerig, *J. Chem. Phys.* **1995**, *103*, 3341, and references therein.

  0570-0833/00/3903-0526 $ 17.50+.50/0

[14] P. J. Rousseeuw, *J. Am. Stat. Ass.* **1984**, *79*, 871; M. Ortiz, A. Herrero-Gutierrez, *Chemom. Intell. Lab. Syst.* **1995**, *27*, 231.
[15] H. Friebolin, G. Schilling, L. Pohl, *Org. Magn. Reson.* **1979**, *12*, 569.
[16] J. A. Katzenellenbogen, S. B. Bowlus, *J. Org. Chem.* **1973**, *38*, 627; W. Kroutil, M. Mischitz, K. Faber, *J. Chem. Soc. Perkin Trans. 1* **1997**, 3629; C. Chiappe, A. Cordoni, G. Lo Moro, C. D. Palese, *Tetrahedron: Asymmetry* **1998**, *8*, 341.

Novel Single- and Double-Layer and Three-Dimensional Structures of Rare-Earth Metal Coordination Polymers: The Effect of Lanthanide Contraction and Acidity Control in Crystal Structure Formation**

Long Pan, Xiaoying Huang, Jing Li,* Yonggang Wu, and Nengwu Zheng

The concept of rational design of micro- and mesoporous and other functional materials has attracted much attention because of the potential of these materials in various applications, such as molecular magnets, nonlinear optical devices, catalysts, molecular sieves, and sensors.[1] The construction of coordination networks possessing zeolite- or clay-like structures offers great challenges and opportunities in terms of controlling their shape and size for selective adsorption. Much of the work has so far been focused on coordination polymers containing transition metal (Groups 8 to 10) and post-transition metal (Groups 11 and 12) elements including Fe, Co, Ni, Cu, Ag, Zn, Cd, and Hg. Rare-earth metal compounds have seldom been investigated.[2] To date, no systematic investigation across the lanthanide series with a single ligand has been carried out. Due to their high coordination number and special magnetic and fluorescence properties, the lanthanide series is likely to provide new materials that possess specific properties and desired features. In this communication, we report the hydrothermal synthesis, structures, and properties of six novel lanthanide coordination polymers and the investigation of the effects of lanthanide contraction and solution pH on the crystal structures of these compounds.

Hydrothermal synthesis[3] is an effective and promising method for growing crystals of numerous inorganic compounds. Recently, we and others have successfully grown single crystals of a variety of transition metal coordination polymers using this approach.[4, 5] Our exploratory studies also show that the hydrothermal environment is suitable for preparation of lanthanide compounds.

In this work, we have chosen a single, multifunctional ligand, 3,5-pyrazoledicarboxylic acid (H_3pdc, **1**), based on the following considerations: a) it has multiple coordination sites

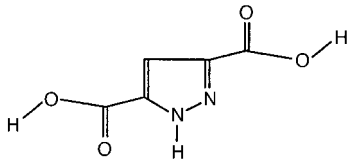

1

that allow structures of higher dimensions; b) it has an asymmetric geometry that may lead to acentric crystal structures; and c) it has abstractable protons that allow various, acidity-dependant coordination modes. In general, the lanthanide series can be divided into three groups according to their masses: the lighter La – Pm (Group 1), the intermediate Sm – Dy (Group 2), and the heavier Ho – Lu (Group 3). Representative metals from each Group were selected and investigated.

In a typical reaction 0.25 mmol of rare-earth metal(III) nitrate and 0.25 mmol of **1** in 10 mL H_2O was used. The mixture was placed into a 23 mL acid-digestion bomb lined with Teflon and heated at 150 °C for 3 days. Reactions with Group 1 lanthanide nitrates $Ln(NO_3)_3$ (Ln = La, Ce) generated $[Ln_2(Hpdc)_3(H_2O)_4]\cdot 2H_2O$, Ln = La (**2**), Ln = Ce (**3**). Group 2 nitrate $Eu(NO_3)_3$ produced $[Eu_2(Hpdc)_3(H_2O)_6]$ (**4**) and a minor product $[Eu_2(Hpdc)_3(H_2O)_4]\cdot 2H_2O$ that is isostructural to **2** and **3**, while Group 3 nitrates $Ln(NO_3)_3$ (Ln = Er, Lu) yielded $[Er_2(Hpdc)_3(H_2O)_6]$ (**5**), and $[Ln(Hpdc)(H_2pdc)(H_2O)_2]$, Ln = Er (**6**), Ln = Lu (**7**).

Single-phase polycrystalline samples of both **2** and **3** were obtained with 68% and 71% yields, respectively. Both compounds are stable in air and are not soluble in any common solvents. Single crystal X-ray diffraction analyses were performed on selected crystals of both compounds. Their crystal structures[6] are isotypic with a three-dimensional framework (see Figure 1a) containing nine-coordinate lanthanide metal centers. There are two types of metal environments in this structure. As shown in Figure 1b, three $Hpdc^{2-}$ ligands chelate to Ln1 through a carboxylate oxygen and adjacent nitrogen atoms (O3/N2, O5/N3, O9/N5), occupying six coordination sites of Ln1. The remaining three coordination sites of Ln1 are taken by another three $Hpdc^{2-}$ ligands, each through a single carboxylate oxygen atom (O2, O7, O12). The second metal environment has Ln2 bonding to a chelated carboxylate group of a $Hpdc^{2-}$ ligand (O1, O2) and to three carboxylate groups of three additional $Hpdc^{2-}$ ligands (O5, O9, O11). The remaining four coordination sites are occupied by the oxygen atoms of four water molecules (O13, O14, O15, O16). There are three crystallographically independent $Hpdc^{2-}$ molecules in the structure, each having a different coordination mode. The highly unsymmetric coordination pattern of the metal and the ligand led to a crystal structure

[*] Prof. J. Li, L. Pan, X. Huang
Department of Chemistry
Rutgers University, Camden, NJ 08102 (USA)
Fax: (+1) 856-225-6506
E-mail: jingli@crab.rutgers.edu
Y. Wu, Prof. N. Zheng
Department of Chemistry
University of Science and Technology of China
Hefei, Anhui 230026 (P. R. China)

[**] This work was supported by the National Science Foundation (DMR-9553066).

  0570-0833/00/3903-0527 $ 17.50+.50/0